Regular Article

blood

MYELOID NEOPLASIA

NADPH oxidase-2 derived superoxide drives mitochondrial transfer from bone marrow stromal cells to leukemic blasts

Christopher R. Marlein,[1,*] Lyubov Zaitseva,[1,*] Rachel E. Piddock,[1] Stephen D. Robinson,[2] Dylan R. Edwards,[1] Manar S. Shafat,[1] Zhigang Zhou,[1] Matthew Lawes,[3] Kristian M. Bowles,[1,3] and Stuart A. Rushworth[1]

[1]Norwich Medical School and [2]School of Biological Sciences, The University of East Anglia, Norwich Research Park, United Kingdom; and [3]Department of Haematology, Norfolk and Norwich University Hospitals NHS Trust, Norwich, United Kingdom

Key Points

- Functional mitochondria are transferred in vivo from BMSC to the leukemic blast.
- AML-derived NOX2 drives transfer of mitochondria via the generation of superoxide.

Improvements in the understanding of the metabolic cross-talk between cancer and its microenvironment are expected to lead to novel therapeutic approaches. Acute myeloid leukemia (AML) cells have increased mitochondria compared with nonmalignant CD34$^+$ hematopoietic progenitor cells. Furthermore, contrary to the Warburg hypothesis, AML relies on oxidative phosphorylation to generate adenosine triphosphate. Here we report that in human AML, NOX2 generates superoxide, which stimulates bone marrow stromal cells (BMSC) to AML blast transfer of mitochondria through AML-derived tunneling nanotubes. Moreover, inhibition of NOX2 was able to prevent mitochondrial transfer, increase AML apoptosis, and improve NSG AML mouse survival. Although mitochondrial transfer from BMSC to nonmalignant CD34$^+$ cells occurs in response to oxidative stress, NOX2 inhibition had no detectable effect on nonmalignant CD34$^+$ cell survival. Taken together, we identify tumor-specific dependence on NOX2-driven mitochondrial transfer as a novel therapeutic strategy in AML. (*Blood*. 2017;130(14):1649-1660)

Introduction

Acute myeloid leukemia (AML) is characterized by infiltration of the bone marrow by proliferative, clonal, and poorly differentiated cells of the hematopoietic system.[1] AML can occur at any age, but primarily affects the elderly, with an average age at diagnosis of 72 years and three-quarters of patients diagnosed after the age of 60 years.[2] Despite existing cytotoxic treatments directly targeting the leukemic cell, two-thirds of younger adults and 90% of older adults will die of their disease.[3] Moreover, current aggressive chemotherapy regimens are often poorly tolerated by the older, less fit patients. Improved outcomes are expected to be achieved through novel therapies developed from an improved understanding of the biology of the disease.

AML blasts cultured in vitro undergo high levels of apoptosis; however, the tumor rapidly proliferates in vivo, demonstrating that the tissue microenvironment plays a fundamental role in the development of AML disease.[4,5] The bone marrow microenvironment consists of many cell types not directly involved in hematopoiesis.[6] These include endothelial cells, osteoclasts, osteoblasts, adipocytes, and fibroblasts,[7] which are broadly classed as bone marrow stromal cells (BMSC) and have previously been shown to support AML survival and contribute to chemotherapy resistance.[8]

In general, cancer cells depend on aerobic glycolysis to generate adenosine triphosphate (ATP), as hypothesized by Warburg in 1956,[9] and this is thought to be a result of activation of oncogenes that promote glycolysis.[10] However, the metabolism of AML blasts differs from most other cancers in that AML is primarily dependent on mitochondrial oxidative phosphorylation for survival.[11] It is also established that AML cells have higher mitochondria levels compared with nonmalignant hematopoietic stem cells,[12,13] which is entirely consistent with the observations that the tumor is dependent on a mitochondrial ATP production pathway. This proposes a key question: Are the additional mitochondria in the AML blasts generated within the tumor cell, or have they been acquired?

For a long time, mitochondria were thought to be retained in their somatic cell for their lifetime; however, in 2004, the Gerdes laboratory showed that mitochondria can be transferred between cells.[14] The main cell type in the bone marrow microenvironment, BMSC, have been shown to donate their mitochondria to lung epithelial cells, preventing acute lung injury.[15] More recently, BMSC have been shown to donate their mitochondria within the bone marrow niche[16]; at this time, however, the mechanisms facilitating mitochondrial transfer in the bone marrow remain poorly defined, and the stimuli for transfer unknown. In the present study, we look to identify the drivers for mitochondrial transfer from BMSC to AML blasts and evaluate the mechanisms through which this occurs. Finally, we address whether blocking this process is lethal to the tumor and what effects such inhibition has on counterpart nonmalignant hematopoietic progenitor cells in the bone marrow.

Methods

Primary cell culture and differentiation

Primary AML blasts were obtained from patient bone marrow after informed consent and under approval from the UK National Research Ethics Service

Submitted 10 March 2017; accepted 14 July 2017. Prepublished online as *Blood* First Edition paper, 21 July 2017; DOI 10.1182/blood-2017-03-772939.

*C.R.M. and L.Z. are joint first authors.

The online version of this article contains a data supplement.

There is an Inside *Blood* Commentary on this article in this issue.

The publication costs of this article were defrayed in part by page charge payment. Therefore, and solely to indicate this fact, this article is hereby marked "advertisement" in accordance with 18 USC section 1734.

(LRCEref07/H0310/146). Nonmalignant $CD34^+$ hematopoietic stem cells were obtained from peripheral blood venesections from patients without leukemia. AML cell isolation was carried out by density gradient centrifugation, using Histopaque (Sigma-Aldrich), and cell type was confirmed by flow cytometry, as previously described.[17] Samples with fewer than 90% blasts were purified using $CD34^+$ microbead selection (Miltenyi Biotec); samples with greater than 90% blasts were not purified. $CD34^+$ hematopoietic stem cells were isolated using density gradient centrifugation and $CD34^+$ microbeads (Miltenyi Biotec). BMSC were isolated from AML patient samples by adherence to tissue culture plastic and were then expanded in Dulbecco's modified Eagle's medium containing 20% fetal bovine serum and supplemented with 1% penicillin-streptomycin (Hyclone, Life Sciences). BMSC markers were confirmed using flow cytometry for expression of $CD90^+$, $CD73^+$, $CD105^+$, and $CD45^-$. BMSC were passaged 3 times before use in the assays presented in this manuscript.

MitoTracker-based mitochondrial transfer assay

Human primary BMSC were stained with 200 nM MitoTracker Green FM for 1 hour. Primary AML blasts were also stained with 200 nM MitoTracker Green FM for 30 minutes before coculture with BMSC to eliminate the possibility dye leakage might be responsible for any increased MitoTracker fluorescence in the AML blast after coculture with the BMSC. Both cell types were washed 3 times in phosphate buffered saline (PBS) to remove the unbound probe. Stained AML blasts were added to stained BMSC at a 5:1 ratio for 24 hours. Stained AML blasts were also grown in monoculture for 24 hours as a control. After incubation, AML blasts were removed from BMSC, and MitoTracker fluorescence in these cells was analyzed using the CyFlow Cube 6 or the Cytoflex flow cytometer, specifically gating on $CD45^+$ cells to exclude contaminating BMSC. Doublets were excluded from the analysis using FSH-A and FSH-H (supplemental Figure 1, available on the *Blood* Web site). This assay was used to quantify mitochondrial transfer to determine the stimulus mechanism; the difference in MitoTracker fluorescence between AML blasts grown with and without BMSC provided a baseline mitochondrial transfer. A pharmacological screen was carried out, whereby drugs and pathway inhibitors (Sigma Aldrich, Cell Signaling, Selleck Chemicals, and Tocris) were added to the MitoTracker-based coculture, using patient AML blasts.

AML xenograft model

All in vivo studies were carried out after approvals from the UK home office and Animal Welfare and Ethics Board of the University of East Anglia. For this study, the NOD.Cg-Prkdcscid IL2rgtm1Wjl/SzJ (NSG) mice (The Jackson Laboratory, Bar Harbor, ME) were housed under specific pathogen-free conditions in a 12/12-hour light/dark cycle with food and water provided ad libitum, in accordance with the Animal (Scientific Procedures) Act, 1986 (UK). Then 2×10^6 primary AML blasts were intravenously injected into nonirradiated 6-8-week-old NSG mice, and 2.5×10^5 OCI-AML3-luc cells were injected, as per the primary blasts, for the NOX2 knockdown (KD) xenograft. Mice injected with OCI-AML3-luc cells were monitored via in vivo bioluminescent imaging (Bruker, Coventry), as previously described.[18] At predefined humane end points, mice were killed (6-12 weeks postinjection), bone marrow was isolated, and engraftment was determined, using human CD33 and CD45 expression. Human AML blasts were purified from the heterogeneous bone marrow by MACS, using CD45 microbeads. This purified human AML blast population was used for the polymerase chain reaction (PCR) and agarose gel electrophoresis. Levels of mitochondria in the purified OCI-AML3-luc populations were achieved using MitoTracker Green FM staining and flow cytometry.

Lentiviral transduction

NOX2 shRNA glycerol stock was purchased from Sigma Aldrich (TRCN0000064588). Lentivirus particles generated using this construct were produced as previously described.[19] Lentiviral stocks were concentrated using Amicon Ultra centrifugal filters, and titers were determined using the Lenti-X quantitative reverse transcription PCR (qRT-PCR) titration kit (CloneTech). Primary AML blasts were plated at a density of 5×10^4/well in a 24-well plate and infected with the NOX2 lentivirus at MOI 30. NOX2 knockdown was confirmed using qRT-PCR.

Apoptosis

Apoptosis of AML blasts and nonmalignant $CD34^+$ hematopoietic stem cells was measured using propidium iodide/AnnexinV (eBiosciences) after coculture with AML blasts, and was quantified using flow cytometry, as previously described.[20]

Mitochondrial respiration

Mitochondrial respiration in AML blasts was assessed using the Seahorse XFp Analyzer, as previously described,[21] and the Seahorse XF Mito stress test kit (Agilent Seahorse Bioscience), according to manufacturer's specifications. Briefly, AML blasts were cultured with or without BMSC and then removed from coculture and plated in poly-D-lysine-coated (Sigma) assay wells at a density of 2×10^5 per well in base media containing 2.5 mM glucose, 0.5 mM carnitine, and 5 mM *N*-2-hydroxyethylpiperazine-*N*′-2-ethanesulfonic acid. Oligomycin (2 μM), carbonyl cyanide-4-(trifluoromethoxy)phenylhydrazone (0.25 μM), and Rotenone (0.5 μM) were added into the injection ports. The experimental template was designed using Wave software for desktop from Seahorse Bioscience. ATP production was monitored by the CellTitre-Glo assay (Promega).

Statistical analysis

We used the Mann-Whitney *U* test, Wilcoxon matched pairs signal rank test, and paired *t* test to compare results between groups. The Mantel-Cox test was used to analyze Kaplan-Meier survival curves. Results with $P < .05$ (denoted by *), $P < .01$ (denoted by **), and $P \leq .001$ (denoted by ***) were considered statistically significant; ns denotes $P > .05$. Results represent the mean ± standard deviation of at least 4 independent experiments. We performed statistical analysis with GraphPad Prism 5 software (GraphPad, San Diego, CA).

Results

BMSC donate their mitochondria to leukemic blasts

As previously reported, human AML blasts have an increased mitochondrial mass compared with nonmalignant $CD34^+$ progenitor cells[12,13] (Figure 1A). To determine whether BMSC support the increase of mitochondria in AML, we examined mitochondrial content after in vitro coculture. Figure 1B shows that AML increase their mitochondrial mass after coculture with BMSC. Next we used 3 different methods to show that BMSC transfer their mitochondria to primary human AML.

First, we assessed mitochondrial transfer between our patient-derived BMSC and primary AML blasts by infecting BMSC with a rLV.EF1.mCherry-Mito-9 Lentivirus for stable production of mitochondria-incorporated mCherry-tagged protein (supplemental Figure 2). Using this, we observed that primary AML blasts, after coculture with these BMSC, acquired the mCherry fluorescence (Figure 1C-D). This demonstrates that mitochondria from the BMSC with the mCherry tag move to the AML blasts.

Second, we used MitoTracker Green FM stain to quantify mitochondria in AML after coculture with BMSC. We incubated both BMSC and AML with MitoTracker Green FM stain for 1 h. The cells were washed twice in PBS and incubated for 4 h. The cells were then cocultured for 24 h and measured for MitoTracker fluorescence, using flow cytometry. Figure 1E shows that AML when cultured with BMSC had significantly more mitochondria than AML cells cultured alone. This was also the case for AML cell lines OCI-AML3, THP-1, MV4-11, and U937 (supplemental Figure 3). All primary AML blasts analyzed consistently acquired mitochondria from multiple primary BMSC samples tested. Furthermore, there was less than 10% variation in mitochondrial transfer between different BMSC samples used ($n = 6$; supplemental Figure 4). To begin to address whether this is a tumor-specific phenomenon, we repeated the experiment, using nonmalignant

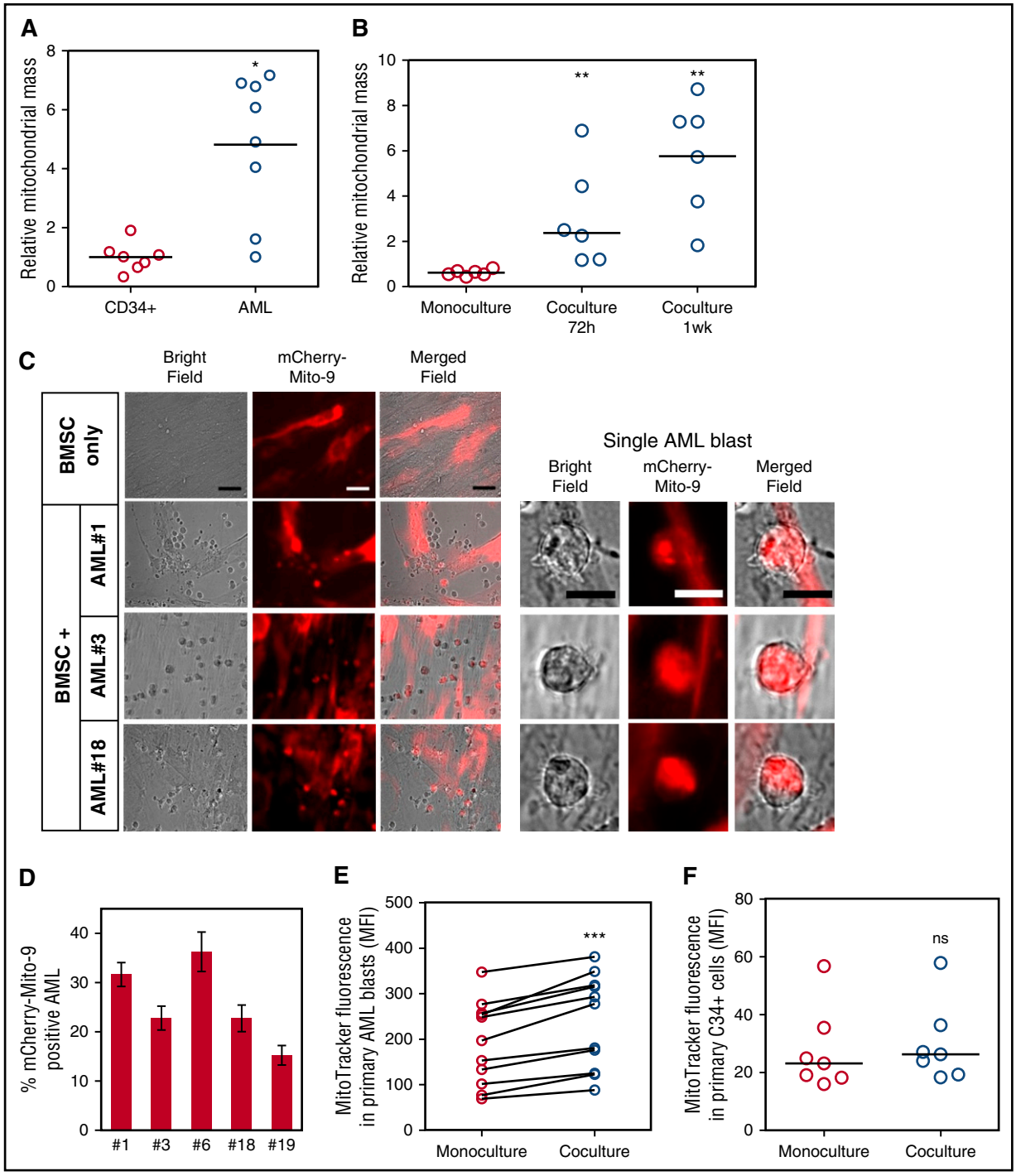

Figure 1. BMSC donate their mitochondria to leukemic blasts. (A) Mitochondrial DNA copy number was assessed in primary nonmalignant CD34$^+$ cells (n = 7) and primary AML blasts (n = 9; P = .0164). (B) Mitochondrial DNA copy number was assessed in primary AML blasts (n = 6) in monoculture vs coculture with BMSC for 72 hours and 1 week (P = .0022). (C) BMSC were transduced with a rLV.EF1. mCherry-Mito-9 Lentivirus. AML blasts were cultured on mCherry-Mito-9 positive BMSC and were analyzed by live cell imaging after a 1-week culture. Bright field, mCherry-Mito9, and merged channels are shown for BMSC only and 3 primary AML patient samples. (Scale bar = 10 μm.) (D) Live cell imaging was repeated with 5 primary AML patient samples; the percentage of mCherry positive AML blasts is presented. (E-F) Primary AML blasts (n = 11) or nonmalignant CD34$^+$ cells (n = 7) were prestained with 200 nM MitoTracker Green FM for 24 hours on BMSC stained with MitoTracker Green FM. MitoTracker fluorescence was analyzed in the AML blasts and nonmalignant CD34$^+$ cells by flow cytometry. A Wilcoxon matched pairs signed rank test was used to determine significance; $P \leq .001$ for the AML blasts and $P > .05$ for the nonmalignant CD34$^+$ cells.

CD34$^+$ cells in the BMSC assay, and showed no significant increase in MitoTracker fluorescence in the hematopoietic progenitor cells (Figure 1F).

Third, we used an in vivo xenograft model in which human primary AML was transplanted into NSG mice. After tumor engraftment, we determined whether mouse mitochondrial DNA (mtDNA) could be detected in the human leukemia cells after extraction from NSG bone marrow. Four individual patient AML samples were transplanted into 8 NSG mice, and after engraftment at between 6 and 12 weeks, human AML blasts were isolated via human CD45 sorting (Figure 2A).

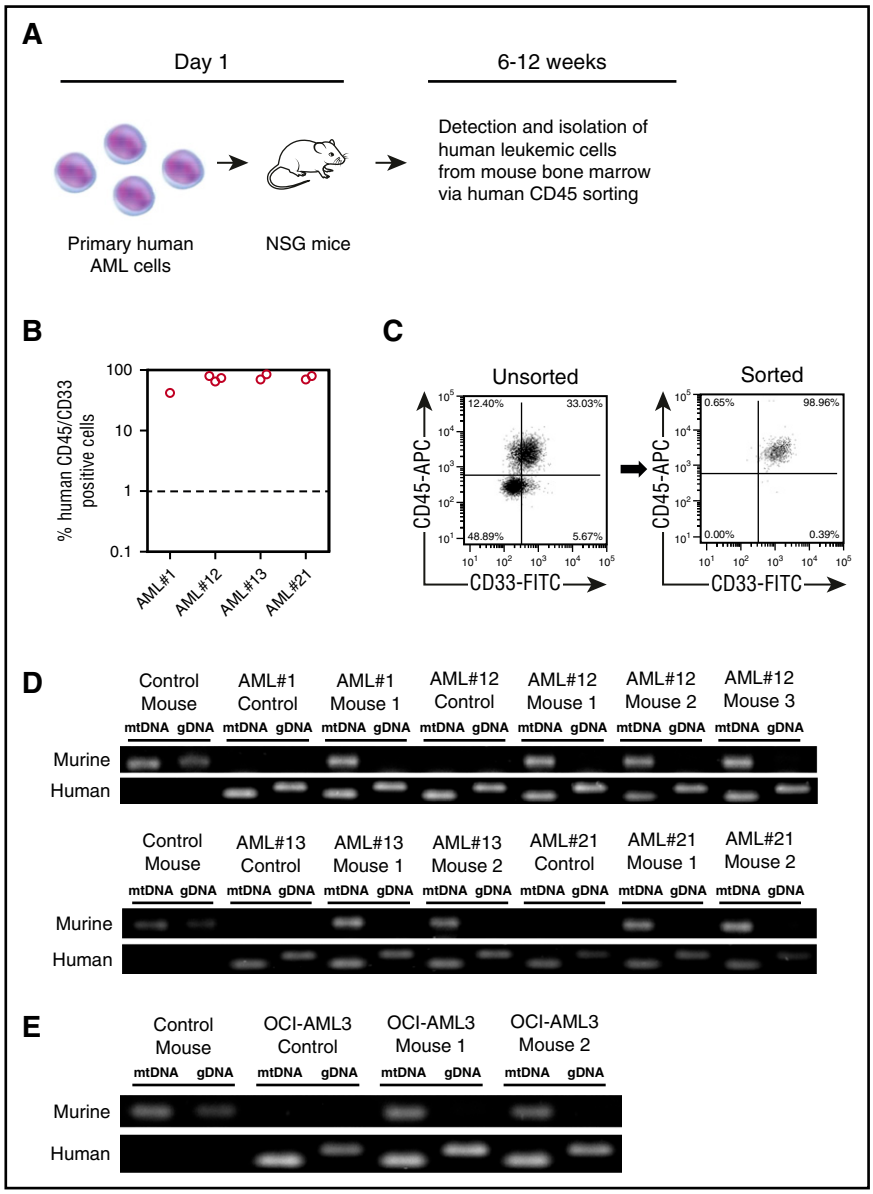

Figure 2. Human AML acquire mouse mitochondria in NSG xenograft model. (A) Schematic representation of patient-derived xenograft model used for these experiments. (B) Into NSG mice, 2×10^6 primary AML cells (4 individual patients with AML) were injected intravenously. Engraftment was measured using human CD33 and human CD45. In the dot plot, each AML engraftment into NSG mice is shown for bone marrow and spleen. (C) Engrafted AML were purified from the mouse BM using human CD45 cell sorting. Shown in the flow figure are unsorted and sorted AML populations from the xenograft. (D) Total DNA was extracted from the purified AML and analyzed by PCR for murine and human specific mitochondrial and genomic DNA. PCR products were visualized by agarose gel electrophoresis. (E) OCI-AML3 cells engrafted into NSG mice were also analyzed by PCR and agarose gel electrophoresis.

Primary AML blasts reliably engrafted into NSG mice, verified by human CD33 and CD45 expression confirming human AML blast identity (Figure 2B). Figure 2C shows that the dual-expressing human $CD45^+/CD33^+$ sorted cells were of 98.96% purity (with $CD45^+/CD33^-$ cells, 0.65%; $CD45^-/CD33^+$ cells, 0.39%; and $CD45^-/CD33^-$, 0.00%). Next, we wanted to determine whether the engrafted AML and subsequent $CD45^+/CD33^+$ purified human blasts had acquired mouse mitochondria. To do this, we performed a PCR-analyzing mouse mitochondrial DNA and mouse genomic DNA. Figure 2D shows that AML blasts isolated from engrafted NSG mice contained mouse mitochondrial DNA, but not mouse genomic DNA; this was also the case for the OCI-AML3 cell line (Figure 2E). As we considered dual expression of CD45 and CD33 to be the more stringent demonstration of human cell purity after the sort, and to examine the potential consequence of murine mtDNA in the assay, we deliberately spiked human DNA (98.96%) with mouse DNA (1.04%) and repeated the PCR. The spiked sample did not create the same result as our mitochondrial transfer assay (supplemental Figure 5) and excludes contamination as the cause of murine mtDNA in the assay. Taken together, these 3 methods show that mitochondria are transferred from BMSC to leukemic blasts both in vitro and in vivo.

Mitochondria transfer occurs via leukemia-derived tunneling nanotubes

A constant observation from live cell imaging was that AML blasts that acquire the mCherry fluorescence are in direct contact with the BMSC. This led us to investigate whether a cell–cell interaction is the way mitochondria move between the 2 cell types (Figure 1C). We first hypothesized that tunneling nanotubes (TNTs) facilitate mitochondrial transfer from BMSC to AML blasts. To inhibit TNT formation, we added cytochalasin B to our mCherry-Mito-9 BMSC-AML coculture experiment. Cytochalasin B treatment did not affect AML or BMSC viability in this assay (supplemental Figure 6). Figure 3A-B shows there is a significant reduction in the percentage of AML blasts that acquire the mCherry fluorescence after cytochalasin B treatment, consistent with mitochondria transfer being from BMSC to AML blast via TNTs.

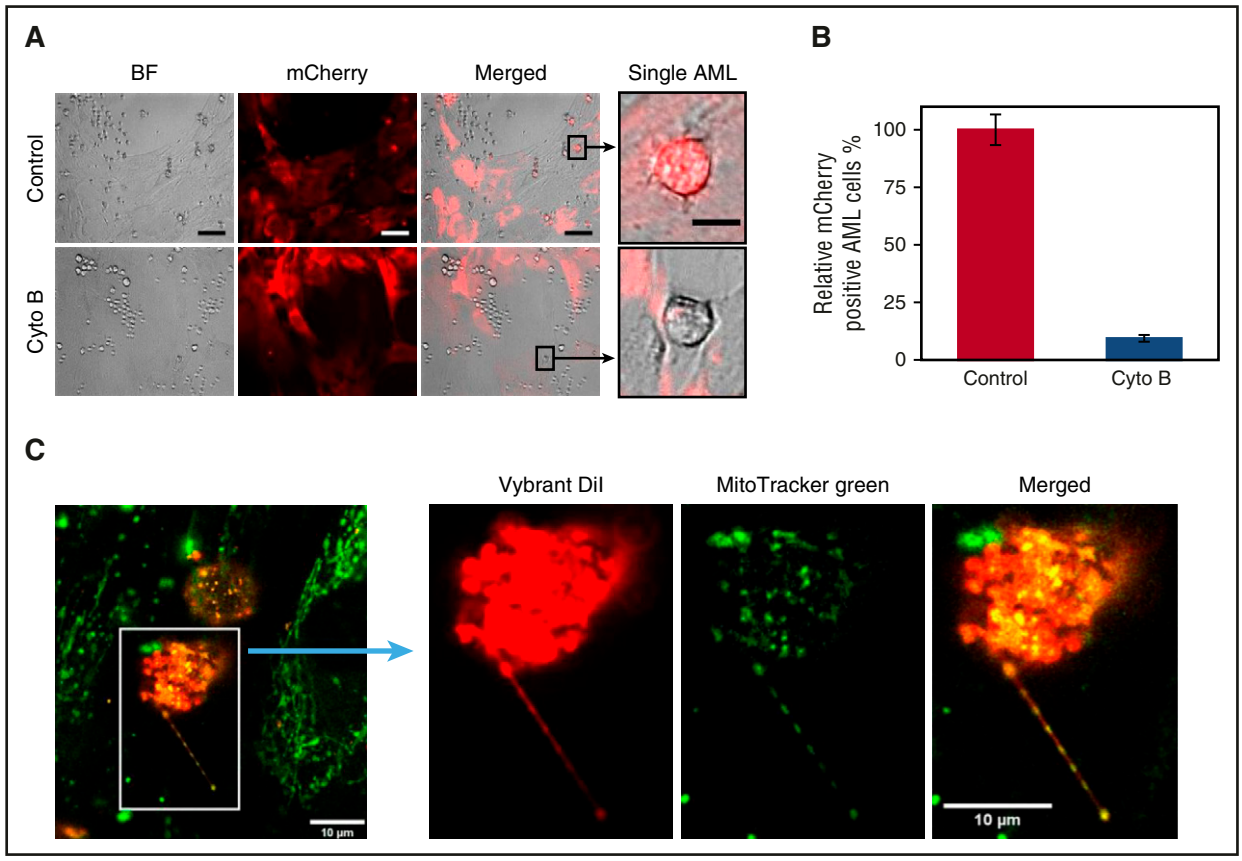

Figure 3. Mitochondria transfer to leukemic blasts occurs via TNT. (A) BMSC were transduced with a rLV.EF1. mCherry-Mito-9 Lentivirus. AML blasts were cultured on mCherry-Mito-9 positive BMSC and were analyzed by live cell imaging. With and without cytochalasin B. (Scale bar, 10 μm.) (B) Multiple primary AML blasts were cultured on rLV.EF1. mCherry-Mito-9 Lentivirus transduced BMSC with and without cytochalasin B; the percentage of mCherry positive AML is shown. (C) AML blasts were stained with Vybrant DiI for 1 hour and washed 3 times in PBS. BMSC were stained with MitoTracker green FM for 1 hour and washed 3 times in PBS. AML blasts and BMSC were then cocultured for 24 hours before fixation, using paraformaldehyde. Cells were visualized by confocal microscopy.

TNTs are functionally dynamic, so to visualize the transfer of mitochondria, we used fixed cell-based imaging. To do this, we stained AML blasts with the Vybrant lipid stain (red) and the mitochondria in BMSC cells with MitoTracker Green FM stain and then cultured the cells together for 24 hours. After coculture, the cells were fixed and TNT formation was detected using confocal microscopy. In Figure 3C, we observed green mitochondria from the BMSC in the red TNT projecting from the AML blasts.

To assess the number of TNT connections occurring in a 24-hour coculture between AML blasts and BMSC, we counted TNT anchor points (TAPs) on fixed cells. These points we describe as residual vybrant diI stain remaining from an AML-derived TNT contact on BMSC. We observe, with 4 AML primary samples, a median of 303 (range, 289-367) TAPs per confocal image (supplemental Figure 7). On cytochalasin treatment, the number of TAPs was significantly reduced to a median of 131 (range, 66-163) TAPs per confocal image (supplemental Figure 7).

The MitoTracker-based quantification assay was next used to examine whether TNTs were the main mitochondrial transfer method. No mitochondrial transfer was seen to occur when AML was cocultured with BMSC in transwell inserts (supplemental Figure 8A). Previous literature shows that mitochondria can move via endocytosis.[16] We therefore examined the effect of an endocytosis inhibitor, dansylcadaverine, on mitochondrial transfer levels in comparison with a TNT inhibitor, cytochalasin B. supplemental Figure 8B shows a significant reduction in mitochondrial transfer between cytochalasin B and dansylcadaverine treatment. From these results, we conclude TNTs are the primary mitochondrial transfer method in AML.

ROS regulates the transfer of mitochondria from BMSC to leukemia blasts

It is not known what stimulates mitochondrial transfer in AML or any cancer. Moreover, determination of the controlling stimulus is essential if this biological process is to be exploited therapeutically in the future. To identify the mechanism of mitochondrial transfer in AML, we used a pharmacological screen in which the MitoTracker experiment described in Figure 1 was employed as the screening tool. Figure 4A shows that *N*-acetyl cysteine (NAC), glutathione, and diphenyleneiodonium (DPI) inhibit mitochondrial transfer. In contrast, we observe that hydrogen peroxide (H_2O_2), daunorubicin, and cobalt chloride further enhance mitochondrial transfer from BMSC to AML blasts. Supplemental Figure 9 shows MitoTracker fluorescence did not change in AML blasts after treatment with NAC, glutathione, H_2O_2, or DPI in monoculture. H_2O_2, but not NAC, reduced AML blast viability, but H_2O_2 had no effect on BMSC viability (supplemental Figure 10). In our baseline experimental conditions, mitochondria did not transfer from BMSC to nonmalignant $CD34^+$ cells (Figure 1F). However, the addition of H_2O_2 to the coculture of nonmalignant $CD34^+$ cells and BMSC cocultures induced mitochondrial transfer to the $CD34^+$ cells.

Next we wanted to determine whether AML blasts are responsible for an increase in reactive oxygen species (ROS) levels in BMSC.

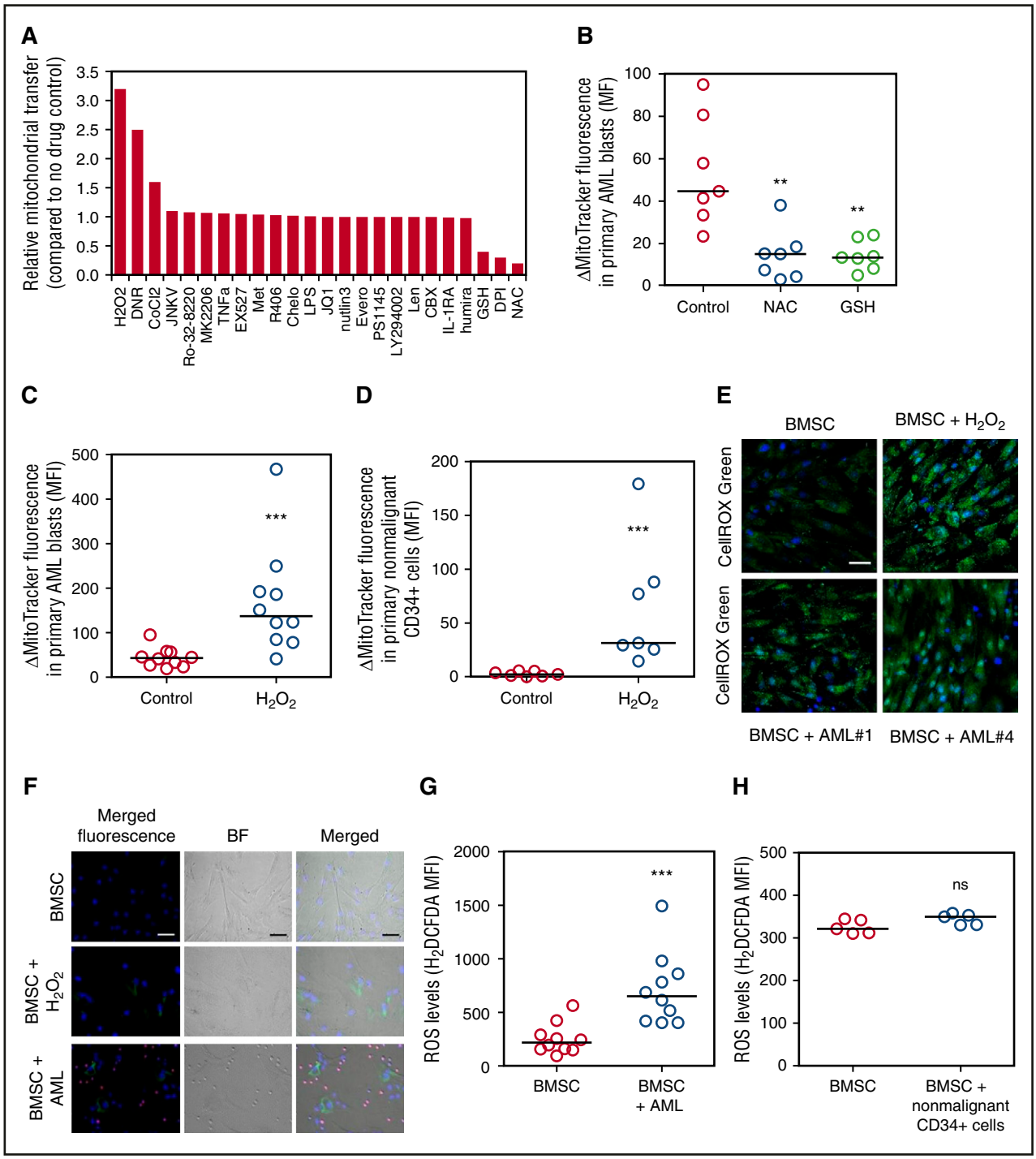

Figure 4. ROS regulate the transfer of mitochondria from BMSC to AML blasts. (A) Primary AML and BMSC were prestained with MitoTracker green FM for 1 hour and then cultured together before 24-hour drug treatment. Flow cytometry was used to detect MitoTracker green FM in the AML blast. (B) Primary AML (n = 7) and BMSC were prestained with MitoTracker green FM for 1 hour and then cultured together before 24-hour NAC (5 mM) and glutathione (5 mM) treatment. Flow cytometry was used to detect MitoTracker green FM in the AML blast. (C) Primary AML (n = 10) and BMSC were prestained with MitoTracker green FM for 1 hour and then cultured together before 24-hour H_2O_2 (50 μM). Flow cytometry was used to detect MitoTracker green FM in the AML blast. (D) Nonmalignant $CD34^+$ cells (n = 7) and BMSC were prestained with MitoTracker green FM for 1 hour and then cultured together before 24-hour H_2O_2 (50 μM). Flow cytometry was used to detect MitoTracker green FM in the nonmalignant $CD34^+$ cells. (E) BMSC cultured alone and in coculture with AML or treated with H_2O_2 (50 μM). AML were removed and BMSC were stained for ROS, using CellROX. BMSC were visualized for ROS, using fluorescence microscopy. (F) BMSC cultured alone and in coculture with AML or treated with H_2O_2 (50 μM) were stained for ROS, using H2DCFDA (10 μM). BMSC were visualized for ROS, using fluorescence microscopy. (G-H) BMSC cultured alone and in coculture with AML (G) or nonmalignant $CD34^+$ cells (H) were stained for ROS, using H2DCFDA (10 μM), and levels were analyzed by flow cytometry.

To do this, we analyzed BMSC ROS when cultured with AML, using 2 assays, CellROX and 2′,7′-dichlorodihydrofluorescein diacetate (H2DCFDA). Figure 4E-G shows that culture with AML blasts causes increased ROS levels and oxidative stress in the BMSC. The increase in ROS in the BMSC is contact-independent, as no significant difference is seen in results between direct contact and transwell coculture

experiments (supplemental Figure 11). ROS levels in BMSC and AML blast cocultures are further increased in hypoxic conditions (supplemental Figure 12A). In addition, there appears to be a positive relationship between ROS levels and the amount of mitochondrial transfer (Pearsons correlation coefficient $R^2 = 0.7455$; $P = .0593$; supplemental Figure 13). Conversely, Figure 4H shows that nonmalignant $CD34^+$ cells do not increase ROS levels in BMSC, and hypoxic conditions do not change this observation (supplemental Figure 12B). Taken together, these results show that AML-induced ROS stimulate mitochondrial transfer from BMSC.

AML-derived NOX2 drives mitochondrial transfer

We observed that DPI was able to inhibit mitochondrial transfer in 2 independent assays (Figure 5A; supplemental Figure 14). As DPI inhibits NOX2, and NOX2-derived ROS plays a critical role in mobilization and homing of nonmalignant hematopoietic stem cells,[22] we next asked whether NOX2-derived superoxide produced by the AML was responsible for mitochondrial transfer. We knocked down NOX2, using a lentiviral transduction (Figure 5B), in 4 human AML patient cell samples and the OCI-AML3 cell line. Then we analyzed mitochondrial transfer to AML after NOX2 or control shRNA knockdown. There is a significant reduction in mitochondrial transfer in the NOX2 KD primary AML cells compared with control KD blasts (Figure 5C), and similarly in the OCI-AML3 cell line (supplemental Figure 15). To confirm superoxide was reduced in the NOX2 KD cells, we analyzed superoxide using the AmplexRED assay. Figure 5D shows that NOX2 KD cells have significantly reduced superoxide. Next we tested whether AML with NOX2 KD could increase ROS in BMSC. Figure 5E shows that NOX2 KD AML cells had a reduced capacity to stimulate ROS production in the BMSC compared with control KD blasts. Finally, we tested whether DPI could reduce survival of AML blasts in culture with BMSC. Figure 5F shows that AML blast survival on BMSC is inhibited by the addition of DPI in coculture. Furthermore, DPI treatment did not cause additional cytotoxicity in monoculture (supplemental Figure 16A). In addition, DPI had little or no effect on the viability of nonmalignant $CD34^+$ cells grown in coculture with BMSC (Figure 5G) or in monoculture (supplemental Figure 16B). Taken together, in leukemic blasts, NOX2-derived superoxide stimulates ROS generation in BMSC, which results in protumoral mitochondrial transfer from the stroma.

Mitochondria acquired by the AML blast are functionally active and contribute to the metabolic capacity

We next explored the function of mitochondrial transfer in relation to mitochondrial respiration. We found that after coculture with BMSC, AML blasts have increased basal and maximum mitochondrial respiration compared with control cells (Figures 6A-B). To help rule out other causes of higher OXPHOS activities in cocultured AML cells, we repeated the experiment with a conditioned media control and observed no significant differences in the mitochondrial respiration between conditioned and nonconditioned media (supplemental Figure 17A). ATP production capacity of AML blasts in coculture with BMSC is also increased compared with control cells (Figure 6C). Finally, we analyzed the mitochondrial respiration in the control and NOX2 knockdown primary AML blasts in coculture with BMSC. We found that knockdown blasts had significantly reduced basal and maximum mitochondrial respiration (Figure 6D). Conversely, NOX2 knockdown had no effect in equivalent monoculture assays (supplemental Figure 17B). Taken together, these data show that mitochondria in AML after coculture with BMSC are functional and contribute to the energy requirements of the rapidly proliferating cancer cell.

NOX2 and the development of AML in an in vivo xenograft model

To analyze the effect of NOX2 on mitochondrial transfer and disease progression, we engrafted control KD and NOX2 KD OCI-AML3-luc cells into NSG mice. Mice were imaged using bioluminescence at weekly intervals. These images revealed there is reduced AML disease progression and engraftment in the bone marrow with NOX2 KD cells compared with the control KD cells (Figure 7A). Furthermore, survival of mice transplanted with NOX2 KD cells was significantly increased compared with those transplanted with the control KD cells (Figure 7B). The growth capacity and cell viability in in vitro monoculture was unaltered between the control KD and NOX2 KD OCI-AML3 cells (supplemental Figure 18).

OCI-AML3-luc reliably engrafted into NSG mice, verified by human CD45 expression confirming human AML blast identity (Figure 7C). Mitochondrial levels were analyzed in the 2 cell populations pre- and postengraftment into the NSG mice, using MitoTracker Green FM. There was no difference in the mitochondrial levels between the control and NOX2 KD preengraftment (Figure 7D). However, in the purified OCI-AML3-luc cells postengraftment, the control KD cells had significantly increased mitochondrial levels compared with NOX2 KD cells (Figure 7E). Taken together, these results identify an in vivo, functional, protumoral role for NOX2-driven mitochondrial transfer in AML.

Discussion

In this study, we report that BMSC within the protective microenvironment of AML transfer their mitochondria to AML blasts. Furthermore, we show that mitochondria are transferred via AML-derived TNTs. We identified that AML-derived ROS drives mitochondrial transfer from the BMSC to the AML. Specifically, NOX2-derived superoxide generated from the AML causes mitochondrial transfer, which we show through in vitro and in vivo studies. We were able to reduce mitochondrial transfer using both lentiviral knockdown and pharmacological inhibition of NOX2. Overall, our results provide a first in cancer mitochondrial transfer mechanism, whereby the cancer cell drives transfer through increasing oxidative stress in the nonmalignant donor cell.

Mitochondrial transfer is known to occur in other cancers such as breast,[23] lung,[24] and melanoma.[25] Our work shows in patient-derived AML blast and BMSC samples, using 3 in vitro methods and an in vivo model, that mitochondrial transfer was also observed between the BMSC and the AML blast. The mitochondria that move to the AML are also functionally active, highlighting that the AML blast is using this biological phenomenon to its metabolic advantage.

Mitochondrial transfer as described in the context of both benign and malignant disease appears to occur variably through TNTs,[23,26,27] connection-43 GAP junctions,[15] and/or by endocytosis,[16] depending on the individual disease context. Despite these observations, the driver mechanism or mechanisms are not well understood. Mitochondrial transfer in AML cells lines have been recently described to be via an endocytosis mechanism.[16] TNTs have been described in a hematological environment whereby acute lymphoblastic leukemia cells signal to BMSC through these TNTs, resulting in a release of prosurvival cytokines.[28] A constant observation from our work with primary AML patient samples was that AML blasts that acquired mitochondria were in contact with BMSC. Therefore, we hypothesized that mitochondrial transfer from primary BMSC to the primary AML blasts was via

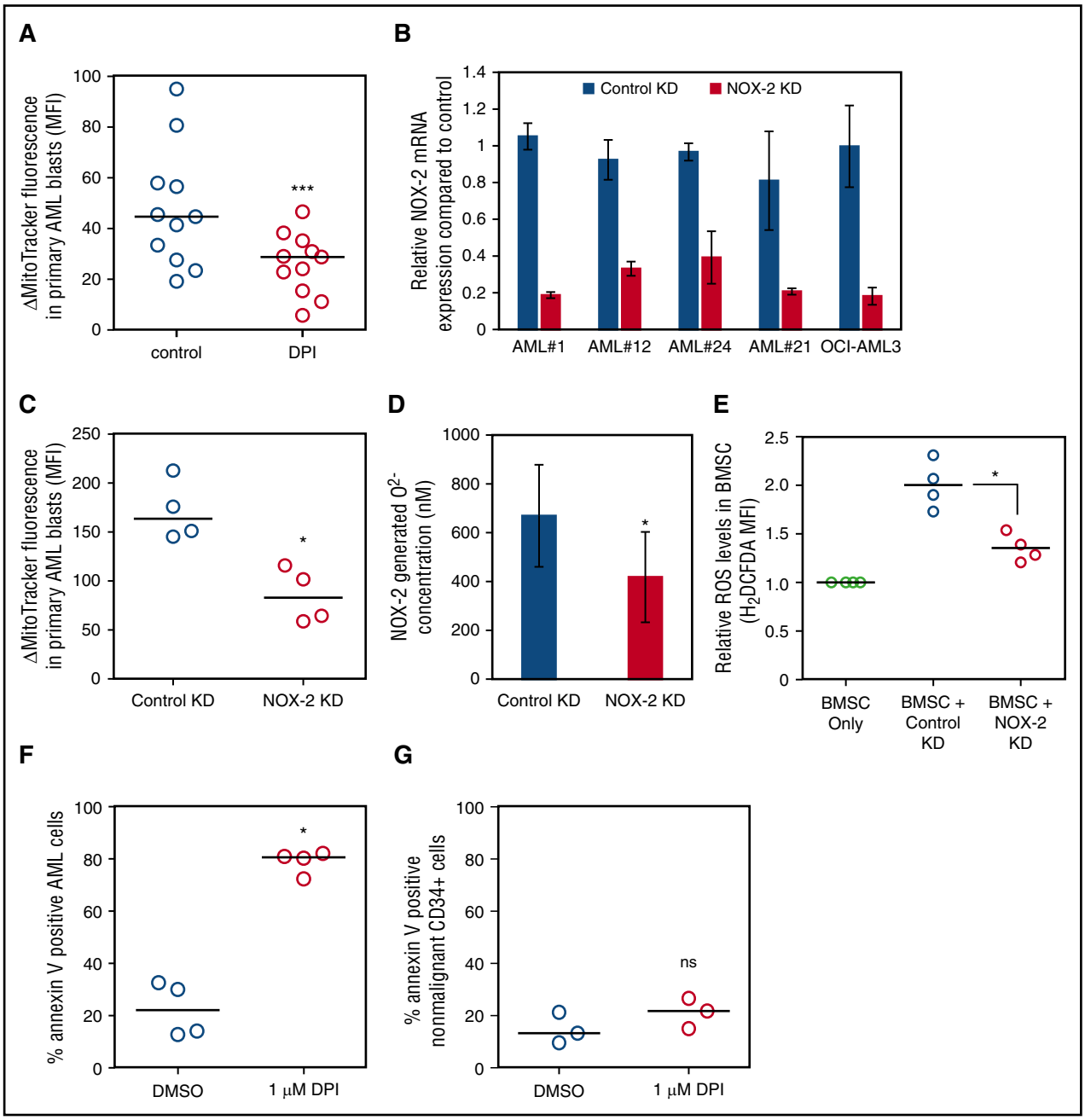

Figure 5. AML-derived NOX2 drives mitochondrial transfer. (A) Primary AML (n = 11) and BMSC were prestained with MitoTracker green FM for 1 hour and then cultured together before 24-hour treatment with DPI (1 μM). (B) Four AML patient samples were transduced with a lentivirus targeted to NOX2 or control for 72 hours. NOX2 mRNA levels were analyzed by real-time PCR and normalized to GAPDH. (C-F) Four AML patient samples were transduced with a lentivirus targeted to NOX2 or control for 72 hours. KD AML cells and BMSC were prestained with MitoTracker green FM for 1 hour and then cultured together for a further 24 hours before MitoTracker was assayed by flow cytometry. (D) Superoxide production was detected in NOX2, and control KD AML cells by AmplexRED assay. (E) BMSC were cultured with control KD AML or NOX2 KD AML. BMSC were stained for ROS, using H2DCFDA (10 μM), and visualized for ROS by flow cytometry. (F) Primary AML or (G) nonmalignant $CD34^+$ were cultured with BMSC and treated with DPI (1 μM) for 72 hours. AML blasts (F) and nonmalignant $CD34^+$ cells (G) were stained with Annexin V and analyzed by flow cytometry.

cell–cell contacts. Through the addition of cytochalasin B to the co-culture and capturing the dynamic interactions through confocal microscopy, we confirmed that mitochondria move from BMSC to AML blasts predominantly through TNTs. Therefore, we believe the primary mitochondrial transfer method is via TNTs.

Through the pharmacological screen, we highlighted that inducing ROS increased mitochondrial transfer, whereas inhibiting ROS reduced transfer. In addition, we found that AML blasts increase oxidative stress in the BMSC. Chronic oxidative stress has been shown to aid tumor survival,[29] metastasis,[30] and proliferation.[31] It is also known that there are high levels of oxidative stress in AML,[32] and that in AML disease relapse, there are increased markers of oxidative stress.[33] As we have shown, oxidative stress drives mitochondrial transfer, and this biological process may be the underlying reason why oxidative stress promotes AML proliferation and relapse. Interestingly using H_2O_2, we could stimulate mitochondrial transfer to nonmalignant $CD34^+$ cells, which do not otherwise acquire mitochondria under our baseline conditions. AML therefore appears to act in a parasitic way by

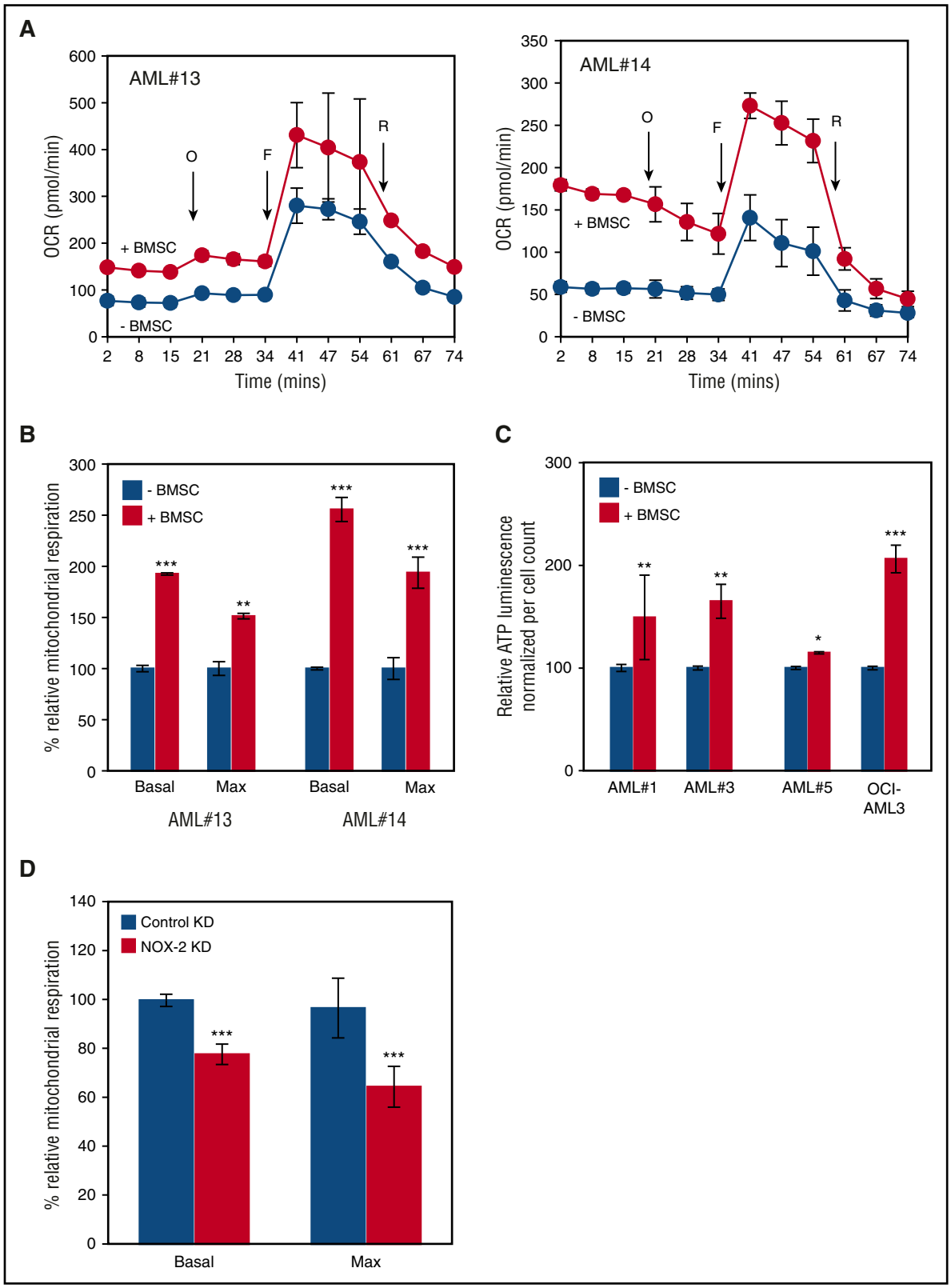

Figure 6. Mitochondria acquired by the AML blasts are functionally active and contribute to the metabolic capacity. (A) Primary AML blasts were grown with and without BMSC for 72 hours and then analyzed independently, using the Seahorse XFp Analyzer with the Mito Stress Test Kit. Data represented as mean ± standard deviation. Sequential injections of Oligomycin (O), carbonyl cyanide-4-(trifluoromethoxy)phenylhydrazone (F), and Rotenone (R) were used to obtain respiration dynamics presented in panel B. (C) Primary AML blasts were grown with and without BMSC, and after 72 hours, the ATP production capacity was analyzed by CellTitre-Glo, with cell numbers normalized. (D) BMSC were cultured with control KD AML or NOX2 KD AML for 72 hours. The blasts were then analyzed, using the Seahorse Extracellular Flux Analyzer; basal and maximum mitochondrial respiration is presented.

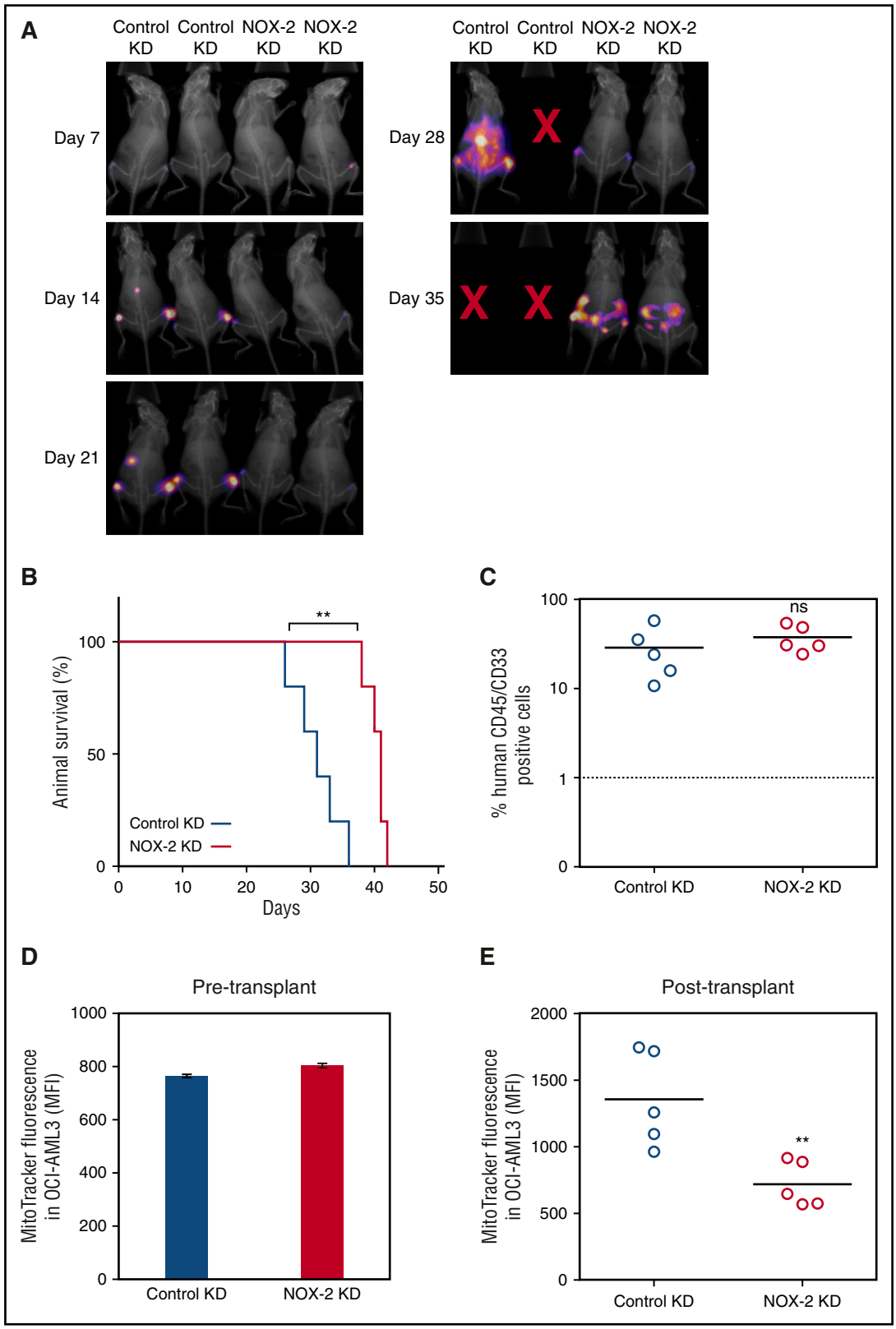

Figure 7. NOX2 and the development of AML in an in vivo xenograft model. (A) Mice were imaged using bioluminescence weekly to monitor engraftment and disease progression in the animals injected with control and NOX2 KD OCI-AML3-luc cells (B) The survival of NSG mice injected with either control KD or NOX2 KD OCI-AML3-luc cells. (C) Engraftment of AML in bone marrow harvested after the human end point was analyzed by flow cytometry for human CD45 expression. (D) Mitochondrial levels were analyzed in the OCI-AML3-luc pre injection into recipient animals by staining for 15 minutes in 200 mM MitoTracker Green FM. (E) Mitochondrial levels in the purified OCI-AML3-luc population after transplant were also analyzed as in panel D.

generating the hypoxic conditions in the bone marrow necessary for mitochondrial transfer from stromal cells.

Moschoi and colleagues[16] found that chemotherapy treatment increases mitochondrial transfer, and we also observed this in our pharmacological screen. Mechanistically, we propose that chemotherapy further increases the already high oxidative stress environment of the bone marrow generated by the AML blast, and thus further increases mitochondrial transfer. This may be clinically relevant in the context of minimal residual disease after chemotherapy treatment. We hypothesize that as a combination of bone marrow hypoxia and chemotherapy, the small population of surviving AML blasts that remain after chemotherapy treatment may have a particularly enhanced quantity of mitochondria. Functionally, this would aid tumor survival and eventually result in relapse. Therefore, targeting this particular mechanism specifically may be theoretically attractive in future strategies aimed at reducing relapse from minimal residual disease.

We show that specifically NOX2 generated superoxide derived from the AML blasts drives the observed mitochondrial transfer, which accordingly provides a molecular target for the process. NOX2 has an established role in immune defense, whereby superoxide produced by NOX2 on phagocytic myeloid cells destroys pathogens.[34] Through DPI drug inhibition of NOX2, we show that in coculture with BMSC, the cell viability of AML blasts is significantly reduced, highlighting the significance of NOX2 in AML disease. NOX2 knockdown blasts have reduced mitochondrial respiration compared with control knockdown cells; therefore, the metabolic requirements of the blasts may not be met, resulting in the observed cell death. Inhibition of NOX2 in vivo highlighted that NOX2 and the resultant mitochondrial transfer is functionally important for AML disease progression, whereby NSG mice administered with NOX2 KD AML outsurvived their control counterparts. Interestingly, in vitro, the cell viability of nonmalignant $CD34^+$ cells is unaffected on the addition of DPI to our coculture experiments. It has been previously described that AML blasts produce a greater quantity of NOX2-derived superoxide than nonmalignant $CD34^+$ cells.[35] This knowledge, combined with the fact that compared with AML, nonmalignant $CD34^+$ cells do not seem to be as dependent on mitochondria from BMSC and do not stimulate such oxidative stress in the BMSC, provides a novel therapeutic window in this disease. We suggest that future strategies targeting mitochondrial transfer from BMSC through NOX2 inhibition may be antileukemic with limited detrimental effects to the normal hematopoietic system.

Overall, we report a first in cancer mitochondrial transfer mechanism whereby NOX2-derived oxidative stress drives transfer from nonmalignant BMSC to AML blasts. Moreover, we show that this mitochondrial transfer is fundamentally a part of the malignant AML phenotype. Accordingly, these results may have the utility to be translated into other malignancies, where mitochondrial transfer has previously been observed but where the specific mechanisms have yet to be elucidated. Finally, our results identify a novel therapeutic opportunity to be developed and explored for the treatment of AML.

Acknowledgments

The authors thank Richard Ball, Mark Wilkinson, Iain Sheriffs, and Sue Steel, Norwich Biorepository (UK) for help with sample collection and storage. pCDH-luciferase-T2A-mCherry was kindly gifted by Irmela Jeremias, MD, from Helmholtz Zentrum München, Munich, Germany.

The authors thank the Rosetrees Trust, The Big C, and the Norwich Research Park Doctoral Training Program for funding.

Authorship

Contribution: C.R.M., L.Z., K.M.B. and S.A.R. designed the research; C.R.M., L.Z., R.E.P., and M.S.S., performed the research; S.A.R., C.R.M., R.E.P., and S.D.R. carried out in vivo work; D.R.E., Z.Z., M.L., and K.M.B. provided essential reagents and knowledge; and C.R.M., L.Z., K.M.B., and S.A.R. wrote the paper.

Conflict-of-interest disclosure: The authors declare no competing financial interests.

Correspondence: Stuart A. Rushworth, Department of Molecular Haematology, Norwich Medical School, University of East Anglia, Norwich NR4 7TJ, United Kingdom; e-mail: s.rushworth@uea.ac.uk; and Kristian M. Bowles, Department of Molecular Haematology, Norwich Medical School, University of East Anglia, Norwich NR4 7TJ, United Kingdom; e-mail: k.bowles@uea.ac.uk.

References

1. Döhner H, Weisdorf DJ, Bloomfield CD. Acute myeloid leukemia. *N Engl J Med*. 2015;373(12):1136-1152.
2. Juliusson G, Antunovic P, Derolf A, et al. Age and acute myeloid leukemia: real world data on decision to treat and outcomes from the Swedish Acute Leukemia Registry. *Blood*. 2009;113(18):4179-4187.
3. Rowe JM, Tallman MS. How I treat acute myeloid leukemia. *Blood*. 2010;116(17):3147-3156.
4. Matsunaga T, Takemoto N, Sato T, et al. Interaction between leukemic-cell VLA-4 and stromal fibronectin is a decisive factor for minimal residual disease of acute myelogenous leukemia. *Nat Med*. 2003;9(9):1158-1165.
5. Rushworth SA, Pillinger G, Abdul-Aziz A, et al. Activity of Bruton's tyrosine-kinase inhibitor ibrutinib in patients with CD117-positive acute myeloid leukaemia: a mechanistic study using patient-derived blast cells. *Lancet Haematol*. 2015;2(5):e204-e211.
6. Shafat MS, Gnaneswaran B, Bowles KM, Rushworth SA. The bone marrow microenvironment - Home of the leukemic blasts [published online ahead of print 12 May 2017]. *Blood Rev*. doi:10.1016/j.blre.2017.03.004.
7. Zimmerlin L, Donnenberg VS, Rubin JP, Donnenberg AD. Mesenchymal markers on human adipose stem/progenitor cells. *Cytometry A*. 2013;83(1):134-140.
8. Abdul-Aziz AM, Shafat MS, Mehta TK, et al. MIF-induced stromal PKCβ/IL8 is essential in human acute myeloid leukemia. *Cancer Res*. 2017;77(2):303-311.
9. Warburg O. On the origin of cancer cells. *Science*. 1956;123(3191):309-314.
10. Düvel K, Yecies JL, Menon S, et al. Activation of a metabolic gene regulatory network downstream of mTOR complex 1. *Mol Cell*. 2010;39(2):171-183.
11. Suganuma K, Miwa H, Imai N, et al. Energy metabolism of leukemia cells: glycolysis versus oxidative phosphorylation. *Leuk Lymphoma*. 2010;51(11):2112-2119.
12. Boultwood J, Fidler C, Mills KI, et al. Amplification of mitochondrial DNA in acute myeloid leukaemia. *Br J Haematol*. 1996;95(2):426-431.
13. Skrtić M, Sriskanthadevan S, Jhas B, et al. Inhibition of mitochondrial translation as a therapeutic strategy for human acute myeloid leukemia. *Cancer Cell*. 2011;20(5):674-688.
14. Rustom A, Saffrich R, Markovic I, Walther P, Gerdes HH. Nanotubular highways for intercellular organelle transport. *Science*. 2004;303(5660):1007-1010.
15. Islam MN, Das SR, Emin MT, et al. Mitochondrial transfer from bone-marrow-derived stromal cells to pulmonary alveoli protects against acute lung injury. *Nat Med*. 2012;18(5):759-765.
16. Moschoi R, Imbert V, Nebout M, et al. Protective mitochondrial transfer from bone marrow stromal cells to acute myeloid leukemic cells during chemotherapy. *Blood*. 2016;128(2):253-264.
17. Zaitseva L, Murray MY, Shafat MS, et al. Ibrutinib inhibits SDF1/CXCR4 mediated migration in AML. *Oncotarget*. 2014;5(20):9930-9938.

18. Vick B, Rothenberg M, Sandhöfer N, et al. An advanced preclinical mouse model for acute myeloid leukemia using patients' cells of various genetic subgroups and in vivo bioluminescence imaging. *PLoS One*. 2015;10(3):e0120925.

19. Rushworth SA, Zaitseva L, Murray MY, Shah NM, Bowles KM, MacEwan DJ. The high Nrf2 expression in human acute myeloid leukemia is driven by NF-κB and underlies its chemo-resistance. *Blood*. 2012;120(26):5188-5198.

20. Piddock RE, Loughran N, Marlein CR, et al. PI3Kδ and PI3Kγ isoforms have distinct functions in regulating pro-tumoural signalling in the multiple myeloma microenvironment. *Blood Cancer J*. 2017;7(3):e539.

21. Shafat MS, Oellerich T, Mohr S, et al. Leukemic blasts program bone marrow adipocytes to generate a protumoral microenvironment. *Blood*. 2017;129(10):1320-1332.

22. Urao N, Inomata H, Razvi M, et al. Role of nox2-based NADPH oxidase in bone marrow and progenitor cell function involved in neovascularization induced by hindlimb ischemia. *Circ Res*. 2008;103(2):212-220.

23. Pasquier J, Guerrouahen BS, Al Thawadi H, et al. Preferential transfer of mitochondria from endothelial to cancer cells through tunneling nanotubes modulates chemoresistance. *J Transl Med*. 2013;11:94.

24. Spees JL, Olson SD, Whitney MJ, Prockop DJ. Mitochondrial transfer between cells can rescue aerobic respiration. *Proc Natl Acad Sci USA*. 2006;103(5):1283-1288.

25. Tan AS, Baty JW, Dong LF, et al. Mitochondrial genome acquisition restores respiratory function and tumorigenic potential of cancer cells without mitochondrial DNA. *Cell Metab*. 2015;21(1):81-94.

26. Lou E, Fujisawa S, Morozov A, et al. Tunneling nanotubes provide a unique conduit for intercellular transfer of cellular contents in human malignant pleural mesothelioma. *PLoS One*. 2012;7(3):e33093.

27. Wang X, Gerdes HH. Transfer of mitochondria via tunneling nanotubes rescues apoptotic PC12 cells. *Cell Death Differ*. 2015;22(7):1181-1191.

28. Polak R, de Rooij B, Pieters R, den Boer ML. B-cell precursor acute lymphoblastic leukemia cells use tunneling nanotubes to orchestrate their microenvironment. *Blood*. 2015;126(21):2404-2414.

29. Clerkin JS, Naughton R, Quiney C, Cotter TG. Mechanisms of ROS modulated cell survival during carcinogenesis. *Cancer Lett*. 2008;266(1):30-36.

30. Wu WS, Wu JR, Hu CT. Signal cross talks for sustained MAPK activation and cell migration: the potential role of reactive oxygen species. *Cancer Metastasis Rev*. 2008;27(2):303-314.

31. Arnold RS, He J, Remo A, et al. Nox1 expression determines cellular reactive oxygen and modulates c-fos-induced growth factor, interleukin-8, and Cav-1. *Am J Pathol*. 2007;171(6):2021-2032.

32. Sallmyr A, Fan J, Rassool FV. Genomic instability in myeloid malignancies: increased reactive oxygen species (ROS), DNA double strand breaks (DSBs) and error-prone repair. *Cancer Lett*. 2008;270(1):1-9.

33. Zhou FL, Zhang WG, Wei YC, et al. Involvement of oxidative stress in the relapse of acute myeloid leukemia. *J Biol Chem*. 2010;285(20):15010-15015.

34. Segal AW, Jones OT, Webster D, Allison AC. Absence of a newly described cytochrome b from neutrophils of patients with chronic granulomatous disease. *Lancet*. 1978;2(8087):446-449.

35. Hole PS, Zabkiewicz J, Munje C, et al. Overproduction of NOX-derived ROS in AML promotes proliferation and is associated with defective oxidative stress signaling. *Blood*. 2013;122(19):3322-3330.